Manuscript submitted April 29, 1986.

Philips Research Laboratories assisted in meeting the publication costs of this article.

REFERENCES

1. H. K. Kuiken, J. J. Kelly, and P. H. L. Notten, *This Journal*, **133,** 1217 (1986).
2. J. J. Kelly and P. H. L. Notten, *Electrochim. Acta*, **29,** 589 (1984).
3. P. H. L. Notten, *ibid.*, **00,** 000 (1986).
4. H. Gerischer, *Ber. Bunsenges. Phys. Chem.*, **69,** 578 (1965).
5. R. Memming, *This Journal*, **116,** 785 (1969).
6. K. Rajeshwar and T. Mraz, *J. Phys. Chem.*, (1983).
7. H. C. Gatos, *Science*, **137,** 311 (1962).
8. K. J. Vetter, "Electrochemical Kinetics," Ch. demic Press, New York (1967).
9. J. J. Kelly and C. H. de Minjer, *This Journal*, (1975).
10. H. Gerischer and I. Wallem-Mattes, *Z. Phys. N.F.*, **64,** 187 (1969).
11. K. W. Frese, M. J. Madou, and S. R. Morrison, *Chem.*, **84,** 3172 (1980).

Chemical Etching Characteristics of InGaAs/InP and InAlAs/InP Heterostructures

Alessandro Stano

CSELT—Centro Studi e Laboratori Telecomunicazioni, 10148 Torino, Italy

ABSTRACT

The chemical etching characteristics of (001) MBE and LPE InGaAs and InAlAs layers grown on InP have been studied for various etching systems: H_3PO_4: H_2O_2, H_2SO_4:H_2O_2:H_2O, and Br_2-CH_3COOH using photoresist as a mask. The etch profiles were examined on stripes oriented along the [110] and [1$\bar{1}$0] directions and on circular mesa structures. The etch rates and the etch-revealed planes are reported, together with a detailed discussion of the crystallography. Experimentally observed different etching characteristics between LPE and MBE InGaAs layers are reported and discussed. The use of these etching solutions for device fabrication is also briefly discussed.

The InGaAs and InAlAs ternary alloys, lattice matched to InP, are currently of great interest for a variety of high speed and optoelectronic devices. Furthermore, they are the two ternary limits of the InGaAlAs quaternary system, which is very promising for fiber and integrated optics applications.

Wet chemical etching and selective chemical etching are important methods in device fabrication. Several etching solutions have been used for InGaAs-based device fabrication: H_2SO_4:H_2O_2:H_2O (1-5) and Br_2-CH_3COOH (6), to define mesa structures for photodiodes, heterobipolar transistors, and for JFET's gate formation, and citric acid and H_3PO_4:H_2O_2:H_2O for JFET's and DH-MESFET fabrication (7-8). Conway *et al.* (9) have reported etch rates for a selective KOH:$K_3Fe(CN)_6$:H_2O etching solution for the InGaAs/InP system. However, to our knowledge, there has been no detailed report on InGaAs and InAlAs etching characteristics, such as device shaping, etch revealed planes, and etch rates, and only limited data on mesa tapering by several different etches have been reported (10).

In this paper, we report detailed experimental results on the chemical etching characteristics of MBE and LPE InGaAs/InP and MBE InAlAs/InP lattice-matched heterostructures in the solutions of three etching systems: (*i*) H_3PO_4, (*ii*) H_2SO_4, and (*iii*) Br_2-CH_3COOH. The etching profiles are examined by cleaving the (001) oriented InGaAs/InP and InAlAs/InP wafers in orthogonal planes along the [110] and [1$\bar{1}$0] directions and are discussed in detail from a crystallographic aspect, together with the etching profiles of circular mesa structures.

Experimental

Sample.—The samples employed were lattice-matched InGaAs and InAlAs heterostructures grown on (001) InP dislocation-free substrates.

The InGaAs samples were grown either by MBE (Si-doped, 10^{18} cm^{-3}), with the growth conditions previously described (11, 12), or by LPE (Sn-doped, 10^{18} cm^{-3}), while the InAlAs samples were grown by MBE (Si-doped, 10^{18} cm^{-3}) (13).

The samples were thinned to about 100 μm to permit cleavage for the observation of the etching profiles. Before mask deposition, the samples were degreased in organic solvents, deoxided in 40% HF, and then rinsed in deionized water.

Masking pattern.—Etching studies were performed on the (001) InGaAs and InAlAs surface after the realization of the masking pattern (see Fig. 1) by standard photolithographic techniques using Hunt HNR 999 negative photoresist baked at 120°C for 30 min.

This geometry allows the simultaneous observation of the etching profiles in the [110] and [1$\bar{1}$0] directions and on circular mesa shapes, where a continuous series of crystallographic planes are present.

Etching solutions.—For device applications, the etching solutions must exhibit oxidizing characteristics and must be free of metallic cations to avoid ionic contamination of the etched surface, which may produce undesired surface current leakage in device applications.

The chemical etching characteristics of InGaAs and InAlAs were studied in the solutions of three etching systems: (*i*) H_3PO_4:H_2O_2, (*ii*) H_2SO_4:H_2O_2:H_2O, and (*iii*) Br_2-CH_3COOH. All the etching experiments were performed at room temperature without stirring. Under these conditions, the first two systems are selective for both the InGaAs/InP and InAlAs/InP heterostructures.

The electronic grade reagents are in the following concentrations: H_3PO_4 (86%), H_2SO_4 (96%), H_2O_2 (33%), CH_3COOH glacial. The etching depths were measured by a

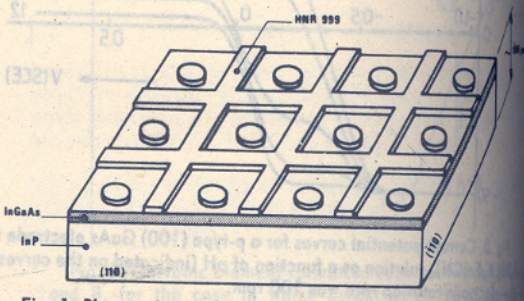

Fig. 1. Photoresist masking pattern on (001) InGaAs or InAlAs surface used for chemical etching experiments.

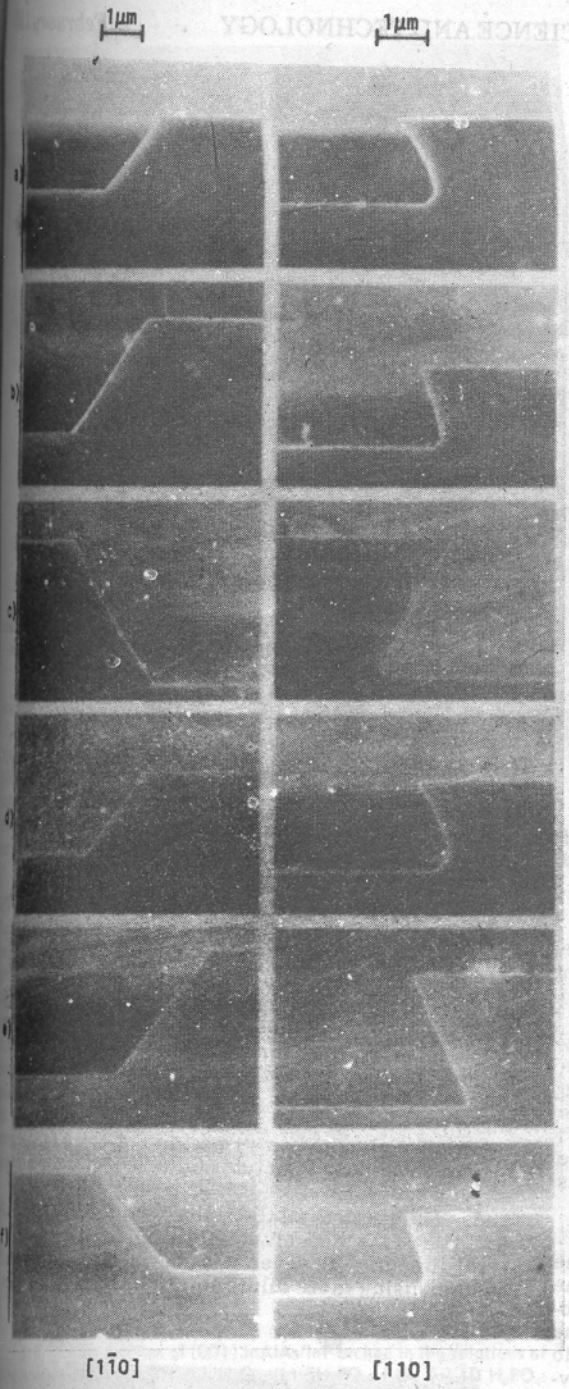

Fig. 2. Etching profiles of (001) InGaAs/InP etched in the solutions of the H_3PO_4 system: (a) $2H_3PO_4$:H_2O_2, (b) $5H_3PO_4$:H_2O_2, (c) 10 H_3PO_4:H_2O_2, (d) H_3PO_4:$8H_2O_2$:H_2O, (e) H_3PO_4:$8H_2O_2$:40 H_2O, and (f) H_3PO_4:$8H_2O_2$:60 H_2O.

step profiler, after mask removal. After etching, the specimens were cleaved along the two directions perpendicular to the (001) surface and then observed in a scanning electron microscope.

InGaAs Etching Profiles

H_3PO_4:H_2O_2 system.—The etching profiles of the (001) InGaAs surface etched in solution of the H_3PO_4:H_2O_2 system are shown in Fig. 2: (a) $2H_3PO_4$:H_2O_2, (b) $5H_3PO_4$:H_2O_2, (c) $10H_3PO_4$:H_2O_2, (d) H_3PO_4:$8H_2O_2$:$1H_2O$, (e) H_3PO_4:$8H_2O_2$:40 H_2O, and (f) H_3PO_4:$8H_2O_2$:60 H_2O.

The resulting etching profiles in the [1$\bar{1}$0] direction, with all the above etching solutions, form an angle of 55° ± 1° with the (001) surface. In the [110] direction, we obtained different profiles, as shown in Fig. 2, which

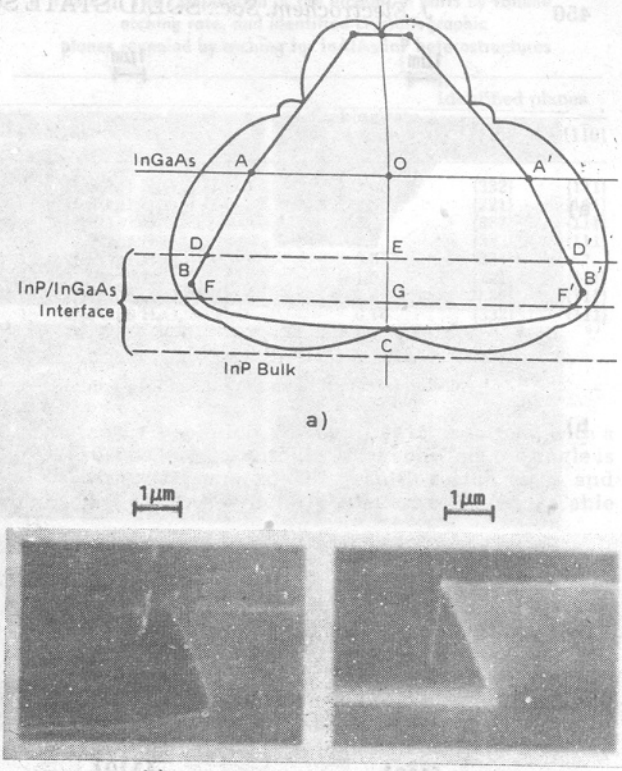

Fig. 3. (a) Polar diagram for InGaAs/InP etching with H_3PO_4:$8H_2O_2$:40 H_2O solution, (b) ABC etching profile, and (c) ADE etching profile.

evolve, with increasing etching time, all in the same way to produce the final shape shown in Fig. 2c and e.

The final profile thus depends on the InGaAs layer thickness and on the etching time but not on the etching solution composition. This behavior can be explained using the etching polar diagram, as discussed by Shaw for GaAs (14, 15), obtained experimentally for the H_3PO_4:$8H_2O$:40 H_2O etching solution and shown in Fig. 3a. Upon increment of the etching time, the obtained etching profiles change from the ABC shape on Fig. 3b to the ABFG shape and to the final ADE shape shown in Fig. 3c. Notice the gradual disappearing of the BC facet, as can be seen in Fig. 3b and c. In the final profile, the resulting [110] surfaces form an angle of 115° ± 1° with the (001) plane. These considerations are valid for all the solutions of the H_3PO_4 and H_2SO_4 systems. The resulting etching time and identified crystallographic planes for all the tested solutions are reported in Table I.

Table I. The composition of the etchant in parts by volume, etching rate for MBE and LPE material, and identified crystallographic planes revealed by etching for InGaAs/InP heterostructures

Etchant		Etching rate (μm/min)		Identified planes	
		MBE	LPE	[110]	[1$\bar{1}$0]
3	H_2SO_4:1 H_2O_2:1 H_2O	2.5	2	{221}	{111}
5	H_2SO_4:1 H_2O_2:1 H_2O	1.9	1.2	{332}	{111}
8	H_2SO_4:1 H_2O_2:1 H_2O	1.2	0.7	{332}	{111}
2	H_3PO_4:1 H_2O_2	3.3	2	{332}	{111}
5	H_3PO_4:1 H_2O_2	2.4	1	{221}	{111}
10	H_3PO_4:1 H_2O_2	0.7	0.5	{332}	{111}
1	H_3PO_4:8 H_2O_2:1 H_2O	1.6	1	{332}	{111}
1	H_3PO_4:8 H_2O_2:40 H_2O	0.4	0.2	{332}	{111}
1	H_3PO_4:8 H_2O_2:60 H_2O	0.2	0.1	{332}	{111}
1%	Br_2-CH_3COOH	6	5	[a]	{112}

[a] Etching profile does not exhibit crystal habits.

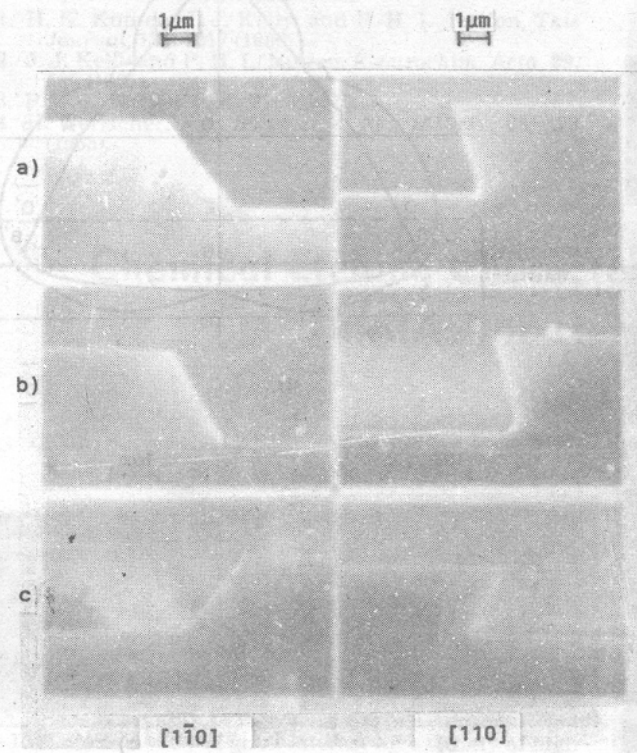

Fig. 4. Etching profiles of (001) InGaAs/InP etched in the solution of the H_2SO_4 system: (a) $3H_2SO_4:H_2O_2:H_2O$, (b) $5H_2SO_4:H_2O_2:H_2O$, and (c) $8H_2SO_4:H_2O_2:H_2O$.

H_2SO_4:H_2O_2 system.—The profiles obtained etching the (001) InGaAs surface in the solution of the H_2SO_4 system are shown in Fig. 4: (a) $3H_2SO_4:H_2O_2:H_2O$, (b) $5H_2SO_4:H_2O_2:H_2O$, and (c) $8H_2SO_4:H_2O_2:H_2O$.

These etching profiles are similar to those previously described for the H_3PO_4 system, since the reaction mechanisms are the same; in the [1$\bar{1}$0] direction, the etching produces a surface that forms an angle of 55° with the (001) plane, while in the [110] direction the angle is 115°. Also, for these etching solutions, the final etching shape in the [110] direction depends on the InGaAs thickness and on the etching time.

Br_2-CH_3COOH system.—Solutions with 1% and 0.1% concentration have been tested. Both solutions show the profiles illustrated in Fig. 5. As can be noted, only in the [1$\bar{1}$0] direction a plane with crystal habit has been obtained with an angle of 38°, which corresponds to the (112) plane. In the [110] direction, the etching profiles do not exhibit clear crystal habits. This is a different behavior from the profiles obtained on InP and InGaAsP, where the same solutions have been tested. For these materials, the etching shape along the [110] direction is found to be dependent on the nature of the mask and on

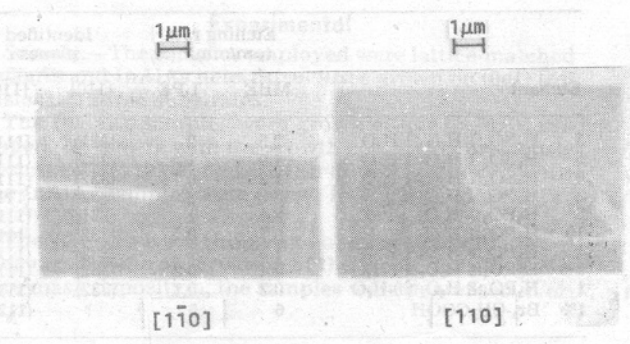

Fig. 5. Etching profiles of (001) InGaAs/InP etched in the solutions of the Br_2-CH_3COOH system: 1% and 0.1% solutions.

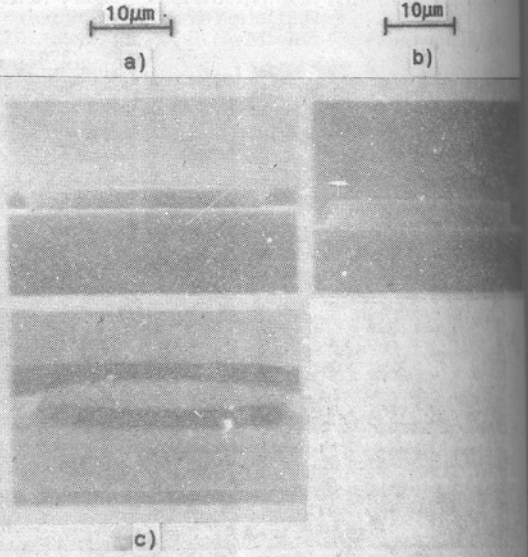

Fig. 6. Etching profiles of (001) InGaAs/InP circular mesa structures (a) H_3PO_4 system, (b) H_2SO_4 system, and (c) Br_2-CH_3COOH system.

the composition of the solution, as it is known for bromine solutions (16).

However, for InGaAs and InAlAs, the profiles always exhibit no clear crystal habit, either with different masks (photoresist, polyimide, Si_3N_4) or with different compositions, independent of etching depth (up to 9 μm). Unlike the two previous etching systems, these solutions are not selective for InGaAs/InP.

InGaAs etching profiles on circular structures.—The etching experiments performed on circular structures should be influenced by all the crystallographic directions that are present on the surface; thus, the etching profile should be gradually varying along the circumference. Actually, the most remarkable effects are in the [110] and [1$\bar{1}$0] directions. For this reason, the real profiles are similar to those obtained on stripes with a gradual variation from the [110] to the [1$\bar{1}$0] direction. Along the [1$\bar{1}$0] direction, all the etching solutions show the same angle obtained on stripes. In Fig. 6, we report some examples of mesa structures obtained with the previous etching solutions.

As can be noted, all the etching solutions of the H_3PO_4 and H_2SO_4 systems always form a negative angle in the [110] direction. However, it is possible that, for the H_2SO_4 system, using more dilute solutions, positive angles or

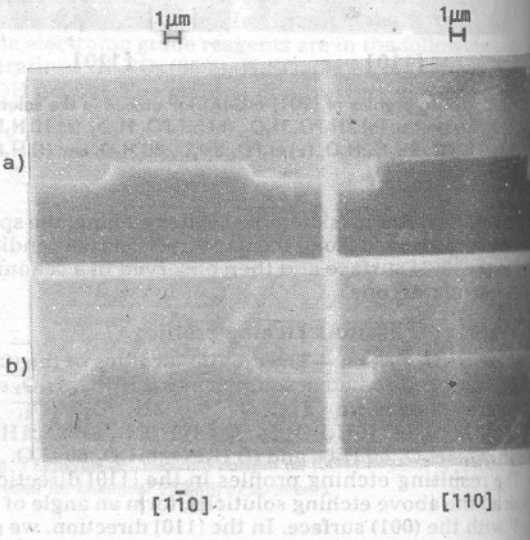

Fig. 7. Etching profiles of (001) InGaAs/InP etched in the solutions of the H_2SO_4 system: (a) $3H_2SO_4:H_2O_2:H_2O$ and (b) $5H_2SO_4:H_2O_2:H_2O$.

Fig. 8. Etching profiles of (001) InAlAs/InP etched in the solutions of the H_3PO_4 system: (a) $2H_3PO_4$:H_2O_2, (b) $5H_3PO_4$:H_2O_2, (c) 10 H_3PO_4:H_2O_2, (d) H_3PO_4:$8H_2O_2$:H_2O, (e) H_3PO_4:$8H_2O_2$:40 H_2O, and (f) H_3PO_4:$8H_2O_2$:60 H_2O.

either crystallographic direction could be obtained, as reported for example in Ref. (4) for a 1:1:20 composition. It can be noted that the only etching solutions that form a positive angle on the [110] and [1$\bar{1}$0] directions are in the Br_2-CH_3COOH system (see Fig. 6c), together with a higher quality surface morphology and with nearly ideal mesa shapes.

InAlAs Etching Profiles

H_2SO_4:H_2O_2 system.—The (001) InAlAs surface has been etched with the following solutions: (a) $3H_2SO_4$:H_2O_2:H_2O, and (b) $5H_2SO_4$:H_2O_2:H_2O. The etching profiles are similar to those obtained for InGaAs, since the reaction mechanisms are the same, and are reported in Fig. 7. In the [1$\bar{1}$0] direction, we have obtained surfaces with an angle of 55°, which belong to the {111} planes, while, in the [110] direction, we obtained two different surfaces:

Table II. The composition of the etchant in parts by volume, etching rate, and identified crystallographic planes revealed by etching for InAlAs/InP heterostructures

Etchant	Etching rate (μm/min)	Identified planes [110]	Identified planes [1$\bar{1}$0]
3 H_2SO_4:1 H_2O_2:1 H_2O	3	{332}	{111}
5 H_2SO_4:1 H_2O_2:1 H_2O	2.5	{221}	{111}
2 H_3PO_4:1 H_2O_2	3	{332}	{111}
5 H_3PO_4:1 H_2O_2	1.5	{332}	{111}
10 H_3PO_4:1 H_2O_2	0.5	{331}[a]	[a]
1 H_3PO_4:8 H_2O_2:1 H_2O	1.5	{221}	{111}
1 H_3PO_4:8 H_2O_2:40 H_2O	0.6	{332}	{111}
1 H_3PO_4:8 H_2O_2:60 H_2O	0.16	{332}	{111}
1% Br_2-CH_3COOH	8	[a]	[a]

[a] Etching profile does not exhibit crystal habits.

with the 3:1:1 solution, an angle of 115° is formed with a {332} surface, while, with the 5:1:1 solution, the angle is 102° with {221} planes. The resulting etch rates and identified crystallographic planes are reported in Table II.

H_3PO_4:H_2O_2 system.—The following solutions have been tested: (a) $2H_3PO_4$:H_2O_2, (b) $5H_3PO_4$:H_2O_2, (c) $10H_3PO_4$:H_2O_2, (d) H_3PO_4:$8H_2O_2$:H_2O, (e) H_3PO_4:$8H_2O_2$:40 H_2O, and (f) H_3PO_4:$8H_2O_2$:60 H_2O. The resulting profiles are collected in Fig. 8, while the etch rates and the identified planes are reported in Table II.

As with the above-mentioned etching solutions, the obtained profiles are formed by {332} and {221} planes in the [110] direction and {111} planes in the [1$\bar{1}$0] direction.

Br_2-CH_3COOH system.—Only the 1% solution has been tested. In this case, unlike that of InGaAs, the obtained etching profiles in the two directions do not reveal a crystal habit, as shown in Fig. 9. The behavior is analogous to that discussed for InGaAs.

InAlAs profiles on circular structures.—The profiles on circular structures reflect those obtained on stripes along the two directions. The resulting mesa shapes for the H_3PO_4 and H_2SO_4 systems are similar to those reported in Fig. 6 for InGaAs and show the presence of

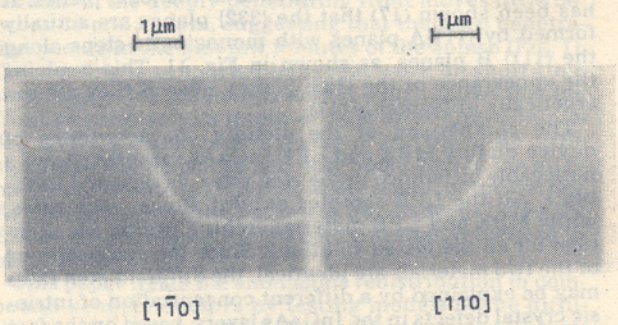

Fig. 9. Etching profiles of (001) InAlAs/InP etched in the solution of 1% Br_2-CH_3COOH.

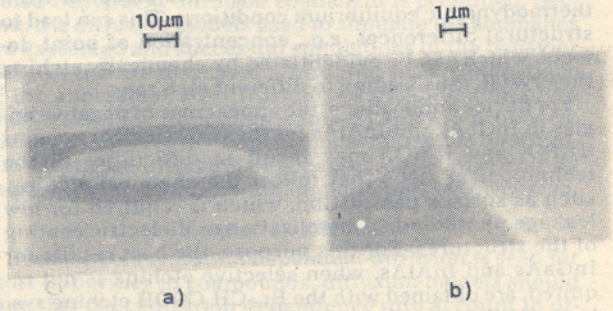

Fig. 10. (a) Etching profiles of (001) InAlAs/InP circular mesa structures etched in the solution of 1% Br_2-CH_3COOH. (b) Magnified view of the InAlAs/InP interface.

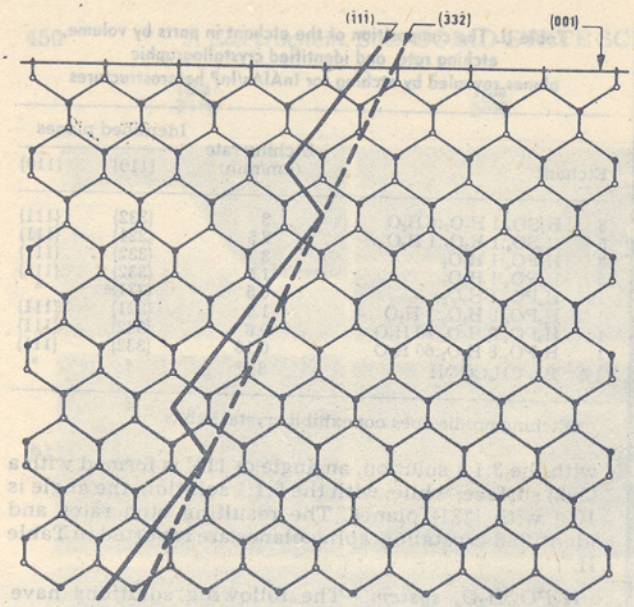

Fig. 11. A (110) section of the zinc blende lattice showing how the {332} surfaces are formed by |111|A planes with monoatomic steps along the |111|B planes.

negative angles. Also, for InAlAs, the best results are obtained with the Br_2-CH_3COOH etching solution, which gives perfectly circular structures with very smooth surfaces, as shown in Fig. 10.

Crystallographic Aspects and Device Applications

The discussion is similar for the two materials; thus, we refer basically to InGaAs. As can be noted from Table I, there is a noticeable uniformity of crystallographic planes revealed by the various etching solutions. The H_3PO_4 and H_2SO_4 systems form with the (001) surface an angle of 55° in the [1$\bar{1}$0] direction, which corresponds to the {111}A planes, with a theoretical angle of 54° 7′ with the (001) surface. In the [110] direction, the angle obtained is 115°, which corresponds to the {332} planes. It has been shown (17) that the {332} planes are actually formed by {111}A planes with monoatomic steps along the {111} B planes, as shown in Fig. 11. This explains the appearance of the {332} planes, even if they are energetically unfavorable (17).

The comparison of the etching characteristics of device-quality MBE and LPE InGaAs samples shows a noticeable difference in the etch rates, as reported in Table I. All the LPE samples exhibit slower etch rates, while MBE and LPE material etching profile are identical for all the tested solutions. Since the compositions of the two materials are identical, the different etch rates may be explained by a different concentration of intrinsic crystal defects in the InGaAs layers, based on the fact that the growth from the liquid phase takes place under thermodynamic equilibrium, while molecular beam epitaxy, as it is widely assumed, takes place far from thermodynamic equilibrium conditions. This can lead to structural differences, *e.g.*, concentration of point defects, which can be evidentiated by chemically etching the crystal, thus leading to different etch rates.

For device applications, the appearance of negative angles in InGaAs and InAlAs for the two selective systems (H_3PO_4 and H_2SO_4) may result in difficulties in the technological steps that follow the chemical etching, such as surface passivation, which is required for low leakage photodiodes, metalization or dielectric coating of the structures. For this purpose, the best results for InGaAs and InAlAs, when selective etching is not required, are obtained with the Br_2-CH_3COOH etching system, which, even if it shows a somewhat high etch rate, has been found to provide a high quality surface morphology, very uniform mesa profiles in both directions with positive angles, and much less sensitivity to the nonuniformities of the etching mask. Recently, low dark current InGaAs photodiodes have been fabricated using this etching solution for mesa definition (12). For InAlAs the etching solutions studied in this work show a further advantage over those solutions previously proposed (10)—they do not require cooling to 4°C to obtain reliable etching characteristics.

The amount of mask undercutting shown by these etching solutions has also to be considered in device fabrication. The Br_2-CH_3COOH system shows an undercutting of half the etching depth with photoresist (PR) and polyimide (PM), and of one third the etching depth with Si_3N_4 masks.

The H_3PO_4 and H_2SO_4 systems show higher undercutting, roughly of the same order of the etching depth using PR and PM masks, slightly less with Si_3N_4.

Conclusions

The chemical etching characteristics of InGaAs/InP and InAlAs/InP heterostructures have been studied in the solutions of three etching systems: H_3PO_4, H_2SO_4, and Br_2-CH_3COOH. The obtained etching profiles, etching rates, and identified crystallographic planes are reported and discussed from a crystallographic and device-applications point of view. Since the results obtained show very similar etching characteristics for InGaAs and InAlAs, it is expected also that the InGaAlAs quaternary system will show analogous characteristics for the compositions between these two ternary limits. The results presented in this study may, therefore, be generalized also to the quaternary alloys.

Acknowledgments

The author wishes to acknowledge C. Papuzza for discussions, P. Cinguino for his continuous support throughout this work, and R. De Franceschi for SEM observations. This work was supported in part by the European Economic Community under the ESPRIT 263 Project.

Manuscript submitted March 12, 1986; revised manuscript received Sept. 11, 1986.

CSELT assisted in meeting the publication costs of this article.

REFERENCES

1. N. Susa, H. Nakagone, O. Mikami, H. Ando, and H. Kanbe, *IEEE J. Quantum Electon.*, **QE-16**, 864 (1980).
2. K. Li, E. Rezek, and H. D. Law, *Electron. Lett.*, **20**, 19 (1984).
3. G. R. Antell and R. F. Murison, *ibid.*, **20**, 919 (1984).
4. H. Dambkes, U. Konig, and B. Schawaderer, *ibid.*, **20**, 955 (1984).
5. D. Wake, A. W. Livingstone, D. A. Andrews, and G. J. Davies, *IEEE Electron Device Lett.*, **EDL-5**, 28 (1984).
6. H. Nickel and E. Kuphal, *J. Opt. Commun.*, **4**, 63 (1983).
7. Y. G. Chai and R. Yeats, *IEEE Electron Device Lett.*, **EDL-4**, 252 (1983).
8. H. Ohno, J. Barnard, C. E. C. Wood, and L. F. Eastman, *ibid.*, **EDL-1**, 154 (1980).
9. K. L. Conway, A. G. Dentai, and J. C. Campbell, *J. Appl. Phys.*, **53**, 1836 (1982).
10. F. Capasso, K. Alavi, A. Y. Cho, and A. L. Hutchinson, *IEEE Electron Device Lett.*, **EDL-5**, 16 (1984).
11. F. Genova, C. Papuzza, C. Rigo, and A. Stano, *J. Cryst. Growth*, **69**, 635 (1984).
12. P. Cinguino, F. Genova, C. Rigo, and A. Stano, *Electron. Lett.*, **21**, 139 (1985).
13. F. Genova, C. Rigo, and A. Stano, Presented at the Third MBE Conference, San Francisco, CA (1984).
14. D. W. Shaw, *J. Cryst. Growth*, **47**, 509 (1979).
15. D. W. Shaw, *This Journal*, **128**, 874 (1981).
16. L. A. Coldren, K. Furuya, and B. I. Miller, *ibid.*, **130**, 1918 (1983).
17. D. N. MacFadyen, *ibid.*, **130**, 1934 (1983).